

Technical Note

Evaluating the Utility of Iron Oxide Nanoparticles for Pre-Clinical Radiation Dose Estimation

Njenga R. Kamau and Michael S. Petronek * 

Department of Radiation Oncology, University of Iowa, Iowa City, IA 52242, USA

* Correspondence: michael-petronek@uiowa.edu; Tel.: +1-(319)-356-8019; Fax: +1-(319)-335-8039

Simple Summary: Radiation readily oxidized Fe^{3+} , which can be used for dosimetric purposes (i.e., Fricke dosimetry). It has recently been discovered that ionizing radiation can oxidize the Fe^{2+} sites of Fe_3O_4 nanoparticles, which can be detected using electron paramagnetic resonance spectroscopy. The goal of this study was to interrogate the utility of Fe_3O_4 nanoparticles as a dosimetric tool. It was discovered that the unique radiochemical properties, particularly the high sensitivity to dose rates, limits the utility of Fe_3O_4 nanoparticles for radiation dosimetry of a pre-clinical external beam irradiator.

Abstract: Nanotechnology has provided considerable advancements in an array of disciplines. Recently, it has been shown that ferumoxytol, a magnetite (Fe_3O_4) nanoparticle, can be oxidized by ionizing radiation. Ferumoxytol nanoparticles have high stability, and thus can be hypothesized that they have dosimetric potential. In this study, it has been observed that xylenol orange, a colorimetric detector of Fe^{3+} used for conventional Fricke dosimetry, was not able to detect radiolytic changes in ferumoxytol. Electron paramagnetic resonance (EPR) spectroscopy was more readily able to evaluate the oxidation of ferumoxytol. EPR spectroscopy revealed that oxidation of 500 nM ferumoxytol in H_2O was linear up to 20 Gy. This concentration, however, was unable to estimate the delivered dose from a Small Animal Radiation Research Platform system, as a 6 Gy dose was estimated to be 1.37 Gy, which represents a 79.2% underestimation of the dose delivered. Thus, while the high stability of Fe_3O_4 nanoparticles is attractive for use in pre-clinical radiation dosimetry, further radiochemical evaluation may be required before considering them for this application.

Keywords: iron oxide nanoparticles; radiation dosimetry; Fricke dosimetry



Citation: Kamau, N.R.; Petronek, M.S. Evaluating the Utility of Iron Oxide Nanoparticles for Pre-Clinical Radiation Dose Estimation. *Radiation* **2024**, *4*, 253–260. <https://doi.org/10.3390/radiation4030020>

Academic Editor: Gabriele Multhoff

Received: 8 August 2024

Revised: 4 September 2024

Accepted: 9 September 2024

Published: 11 September 2024



Copyright: © 2024 by the authors. Licensee MDPI, Basel, Switzerland. This article is an open access article distributed under the terms and conditions of the Creative Commons Attribution (CC BY) license (<https://creativecommons.org/licenses/by/4.0/>).

1. Introduction

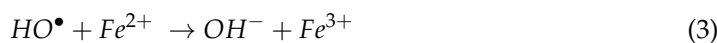
Fricke dosimetry, first invented in 1927, is a dosimetry technique that leverages the radiation-induced oxidation of Fe^{2+} to assess radiation dose delivery [1]. Following the radiolysis of H_2O (Equation (1)):



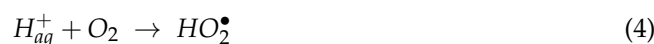
where $\text{H}_2\text{O}^{\bullet+}$ will immediately deprotonate to generate a hydroxyl radical, HO^\bullet (Equation (2)):



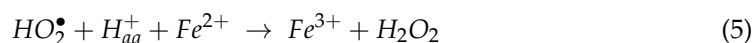
The HO^\bullet generated can readily oxidize Fe^{2+} (Equation (3)):



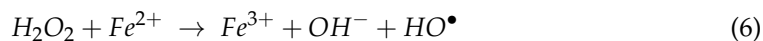
Moreover, the aqueous proton generated, H_{aq}^+ , can react with molecular oxygen (O_2) to generate a hydroperoxyl radical (i.e., protonated superoxide, HO_2^\bullet , Equation (4)):



which can then also go on to oxidize Fe^{2+} (Equation (5)):



The hydrogen peroxide generated is then able to undergo a Fenton reaction (Equation (6)), oxidizing another Fe^{2+} ion:



From this chemistry, the radiolytic yield (i.e., number of Fe^{3+} ions generated per 100 eV of energy deposited, G) can be estimated (Equation (7), [2]):

$$G(Fe^{3+}) = 3G(H^\bullet) + 2G(H_2O_2) + G(HO^\bullet) \quad (7)$$

Thus, Fricke dosimetry directly measures the oxidation of Fe^{2+} in H_2O to estimate radiation doses. Fricke dosimeters are an attractive means of dose estimation because of their relative ease, as they consist of ferrous ammonium sulfate (Fe^{2+}) in H_2O in their simplest form [3,4]. In this case, radiation induces a color shift, changing the solution from a clear-blue solution to a red (Fe^{3+}) solution where the color change, as measured by absorbance or optical density, is directly proportional to radiation dose [5,6]. Fricke dosimeters are also generated by embedding the Fe^{2+} in an agarose gel and measuring optical density changes, which provides the advantage of measuring geometrically accurate dose distributions [3,7–9]. However, despite the advantages of Fricke dosimetry being its ease of use and its simple readout, requiring only an ultraviolet–visible light spectrometer, there are several limitations to this technique, which have hampered its broad utility. Fricke dosimeters are often sensitive to metallic impurities, can lack the sensitivity to measure low-dose radiation (<10–20 Gy), readouts must happen quickly due to ferric ion diffusion or results will be distorted, and ionic diffusion can also cause a distortion of spatial information, leading to inaccurate measurements [6]. Taken together, the lack of stability of traditional Fricke dosimeters suggests that a more stable iteration may be beneficial.

To combat the instability issues associated with traditional Fricke dosimeters, this has led to the investigation of superparamagnetic iron oxide nanoparticles (SPIONs) as a modernized alternative iron-dependent dosimetry technique. SPIONs are highly stable molecules that may exhibit the ability to react with the chemical oxidants generated following the radiolysis of H_2O . As a proof of concept, this study will utilize ferumoxytol (FMX). FMX is a useful tool to test SPION chemistry because it is readily available in a soluble formulation, and thus limiting the burden of chemical synthesis. Most commonly, FMX is a SPION that is FDA-approved to treat iron deficiency anemia, and it is used as a magnetic resonance imaging contrast agent, and it is also a potential cancer therapeutic [10–17]. FMX is a 30 nm SPION with an Fe_3O_4 core (formally, two Fe^{3+} , one Fe^{2+} oxide) encapsulated within a carboxylated polymer coating that can be readily evaluated with electron paramagnetic resonance (EPR) spectroscopy [18]. Much of the work regarding the anti-neoplastic activity of FMX points to its ability to catalyze oxidations and generate ROS [17]. However, robust physicochemical analysis of FMX has been limited. Recently, it has been shown that the Fe_3O_4 core of FMX is, in fact, redox-active and can be decomposed by $AsCH^-$, generating excess cytotoxic levels of H_2O_2 that enhance glioblastoma therapy [19]. This has led to the induction of a phase 1 clinical trial at the University of Iowa testing the safety of FMX as a therapeutic agent in glioblastoma (NCT04900792). Consistent with the redox accessibility of FMX, it has been discovered that ionizing radiation can oxidize the surface charges of FMX in H_2O , resulting in the release of free, catalytically active Fe^{3+} [18]. This effect is radiation dose-dependent much like iron oxidation (i.e., Fricke dosimetry); however, FMX has a unique pattern of radiochemical decomposition that is largely driven by H_2O_2 as opposed to other oxidizing/reducing byproducts of radiation (e.g., HO^\bullet , $O_2^{\bullet-}$, HO_2^\bullet , e_{aq}^-). Moreover, the high stability of the iron oxide lattice gives rise to relatively slow redox kinetics relative to individual iron ions [19]. Therefore, due to the high stability

of iron oxide nanoparticles and their ability to be oxidized by ionizing radiation, it was hypothesized that FMX may serve as a useful tool to evaluate the application of SPIONs for radiation dosimetry.

2. Materials and Methods

2.1. Chemical Preparation and Radiation Delivery

Ferumoxytol (Feraheme[®]; FMX) was diluted to the appropriate concentration from a 30 mg mL⁻¹ stock in either double-distilled H₂O or 0.1 mM xylenol orange (Sigma-Aldrich, St. Louis, MO 52097, USA). Xylenol orange was prepared at an initial concentration of 1 mg mL⁻¹ and titrated to pH = 3.0 before use. Samples were irradiated in solution with a ³⁷Cesium source and a dose rate of 0.6 Gy min⁻¹. Samples were analyzed within 15 min of irradiation unless otherwise specified.

2.2. Electron Paramagnetic Resonance Spectroscopy

FMX oxidation was evaluated by measuring the peak-to-peak signal intensity of the EPR spectra of the low-spin Fe₃O₄ complex at $g = 2$ as previously described [18]. The following scan parameters were used: center field = 3508.97 G, sweep rate = 2000 G/42 s, time constant = 327.68 ms, frequency = 9.85 GHz, power attenuation = 18 dB, modulation frequency = 100 kHz, and modulation amplitude = 0.7 G, with spectra being generated from a signal average of 2 scans.

3. Results

3.1. Evaluation of Xylenol Orange Changes Following Nanoparticle Irradiation

Xylenol orange is a colorimetric indicator that is frequently used to detect iron oxidation as it will turn purple with an absorbance at approximately 585 nm [20,21]. For this reason, xylenol orange is commonly used as an indicator to assess Fricke dosimetry [7,20,21]. Because ionizing radiation has been shown to oxidize the Fe²⁺ sites of Fe₃O₄, decomposition of FMX has been shown to release free Fe³⁺ ions (Figure 1A) [18]; it was initially hypothesized that xylenol orange could serve as a useful tool to evaluate radiation-induced FMX decomposition following a single fraction of 4 Gy. A 4 Gy dose was chosen because FMX radiolysis has previously been shown to be linear up to 10 Gy, and thus 4 Gy would be within the dynamic range of oxidation [18]. However, initial experiments revealed that irrespective of FMX concentration, no xylenol orange color shifts were observed (Figure 1B). Thus, it appears that xylenol orange may not be a useful tool in the context of nanoparticle decomposition following radiation.

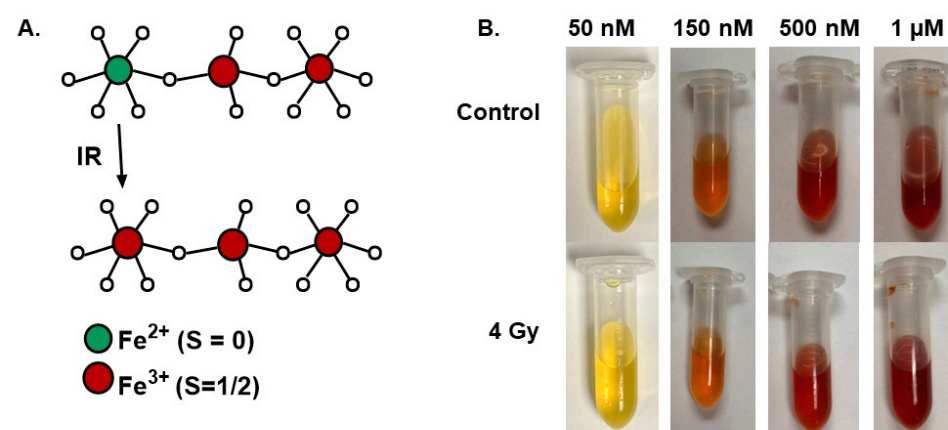


Figure 1. Evaluation of xylenol orange changes following nanoparticle irradiation. (A). Structural schematic of the radio-oxidation of Fe₃O₄. (B). Increasing concentrations of FMX (50 nm–1 μM) were prepared in a 0.1 mM xylenol orange concentration and irradiated with 4 Gy to determine potential colorimetric changes associated with the release of Fe³⁺ from FMX following radiation.

3.2. Electron Paramagnetic Resonance Evaluation of Nanoparticle Irradiation

Because xylenol orange appeared to have insufficient sensitivity to assess FMX nanoparticle decomposition following radiation, changes in FMX structure were evaluated using EPR spectroscopy following a single 4 Gy radiation dose. Consistent with the previous data, FMX EPR signal intensity increased following radiation (Figure 2A) [18]. When performed with multiple FMX concentrations, this effect was only observed at 150 nM and 500 nM concentrations of FMX (Figure 2B,C). Meanwhile, no changes in EPR signal intensity were observed at 50 nM or 1 μ M FMX, suggesting that these concentrations were not optimal for use due to either concentration limitation (i.e., surface charge availability) or signal saturation, respectively.

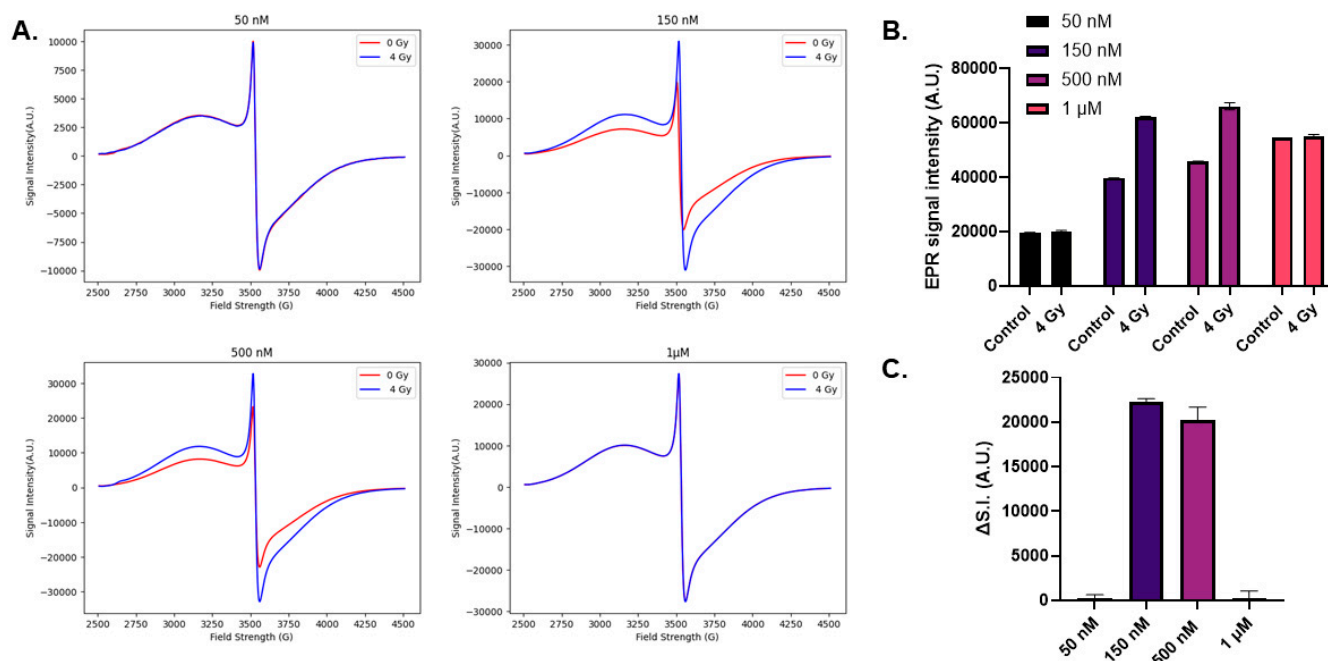


Figure 2. Electron paramagnetic resonance evaluation of nanoparticle irradiation. Increasing concentrations of FMX (50 nM–1 μ M) were prepared in a 0.1 mM xylenol orange concentration and irradiated with 4 Gy and evaluated using EPR spectroscopy. (A) Representative EPR spectra of FMX nanoparticles prior to (blue) and following (red) 4 Gy irradiation. Due to the high iron content of FMX, signal saturation occurred at 500 nM and 1 μ M. Thus, the instrument gain had to be decreased from 5.02×10^4 to 2×10^4 and 1×10^4 , respectively. (B) The peak-to-peak signal intensity of the major, symmetric peak at $g \approx 2$ (≈ 3500 G) was used for quantification. (C) To quantify the effects of 4 Gy on FMX the change in signal intensity ($\Delta SI = SI(4 \text{ Gy}) - SI(0 \text{ Gy})$) was calculated.

3.3. Linearity of Electron Paramagnetic Resonance Spectroscopic Analysis

As it was determined that EPR spectroscopy could detect changes in FMX structure following radiation (4 Gy) at 150 and 500 nM concentrations, this experiment aimed to determine if the radiolytic changes in FMX changes can be used for dose estimation. Both concentrations were evaluated over a range of radiation doses. Previously, it has been reported that FMX radiolysis is linear up to 10 Gy [18]; however, many studies may require doses >10 Gy as many normal tissue injury studies leverage doses up to 20 Gy [22]. Therefore, this study extended the analysis of FMX radiolysis using EPR spectroscopy to up to 20 Gy. When 150 nM FMX was irradiated, EPR signal intensity increased up to 10 Gy; however, no differences were observed from 10 to 20 Gy (Figure 3A). These samples were analyzed 24 h after irradiation to see if any decomposition processes occur overnight; however, it appears that there is little difference in EPR signal intensity. This likely indicates that the surface charges of FMX are initially oxidized and released leaving a slightly smaller nanoparticle when the system returns to equilibrium. Next, 500 nM FMX was

irradiated using the same dose range, and a more linear relationship was observed ($R^2 = 0.9$, slope = 667 A.U. Gy $^{-1}$, Figure 3B). When the system was allowed to reach equilibrium overnight, similar to 150 nM, no differences were observed between radiation doses.

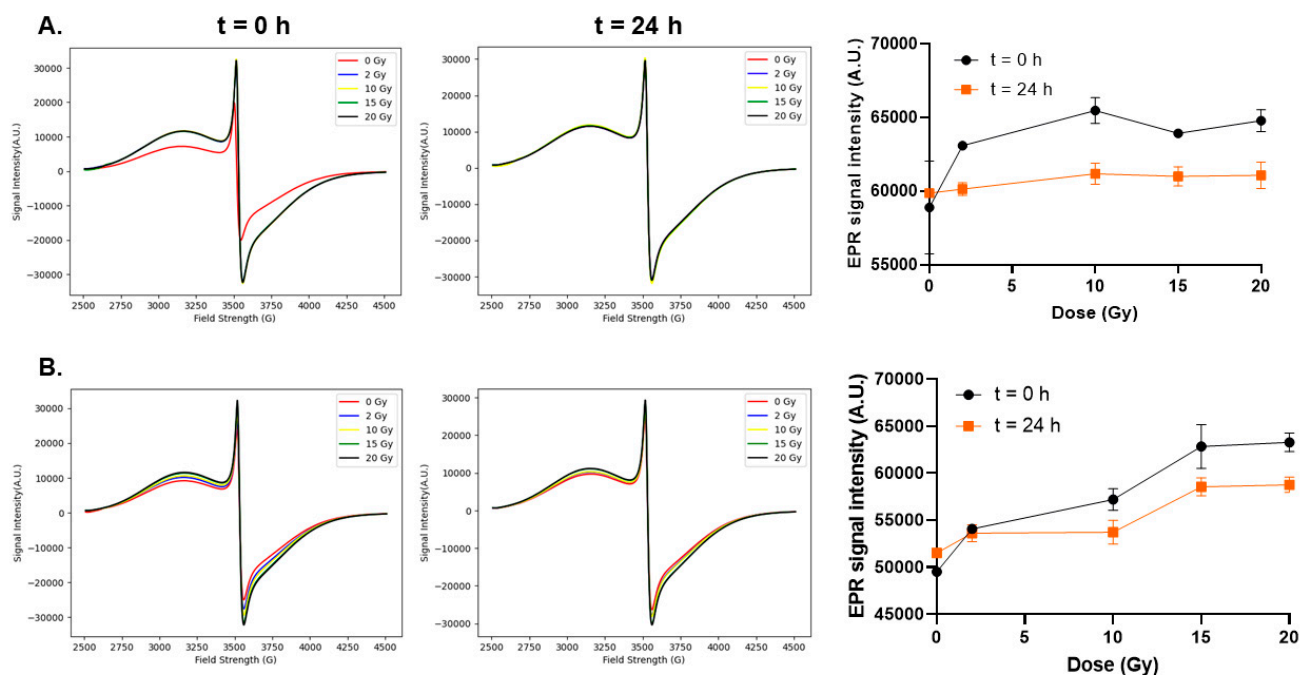


Figure 3. Linearity of electron paramagnetic resonance spectroscopic analysis. FMX nanoparticles in H₂O at 150 nM (A) and 500 nM (B) were irradiated with increasing doses from 0 to 20 Gy and evaluated using EPR spectroscopy. The instrument gain used was 5.02×10^4 and 2×10^4 , respectively.

3.4. Evaluating FMX Radiation Dose Prediction with a Pre-Clinical Irradiation System

Following validation that 500 nM FMX exhibits linearity with radiation doses up to 20 Gy, EPR analysis was used to test whether FMX oxidation could accurately predict the dose delivery from a small animal radiation research platform (SARRP). First, a cone-beam CT image of a 500 nM FMX sample was gathered to generate a treatment plan using the Muriplan software 3.0.0 and prescribe the desired dose of 6 Gy (Figure 4A). Following dose estimation using the Muriplan superposition convolution algorithm, the predicted dose delivered to the sample was 6.25 Gy. Following irradiation, the sample was analyzed using EPR spectroscopy compared to an unirradiated sample to calculate the change in signal intensity (ΔSI , Figure 4B). The ΔSI observed was 850 ± 283 A.U. Using a linear extrapolation method from the previous 0–20 Gy calibration curve (slope = 667 A.U. Gy $^{-1}$), the dose estimate was 1.37 Gy. This estimate is 79.2% lower than the dose prediction generated before irradiation using Muriplan software. As FMX oxidation is highly sensitive to dose rate [18], this major discrepancy may be largely due to the variable dose rates as the ^{137}Cs irradiated samples were performed with a 0.6 Gy min $^{-1}$ beam, and the Xstrahl SARRP for this treatment (S.S.D. ≈ 35 cm) has a dose rate of approximately 2.5 Gy min $^{-1}$. To account for this difference in dose rate, a 3-point calibration curve was generated with the SARRP at this S.S.D., which showed no difference in EPR signal intensity between 10 and 20 Gy (Figure 4C). Therefore, it appears that FMX has limited utility for SARRP-based dosimetry.

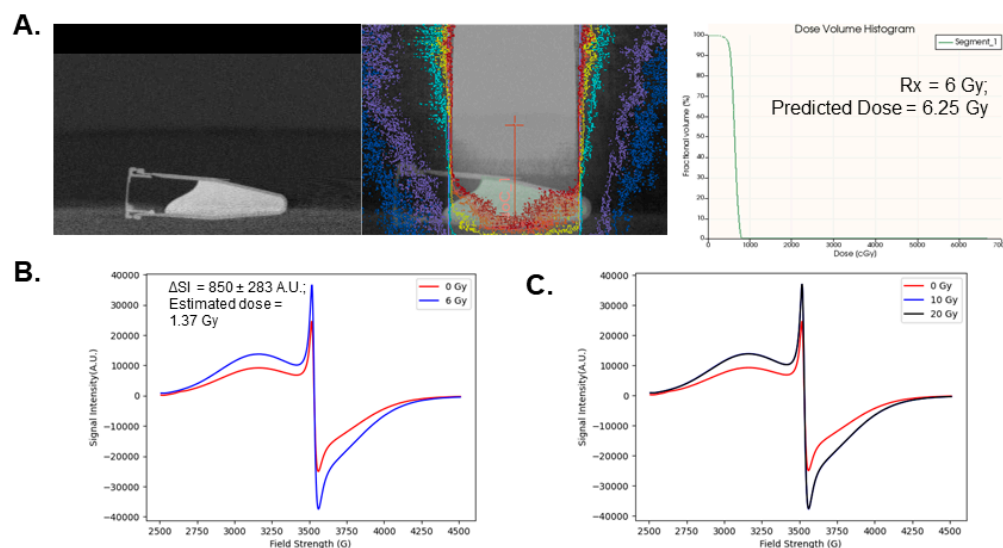


Figure 4. Evaluating FMX radiation dose prediction with a pre-clinical irradiation system. (A). A 500 nM FMX sample was irradiated using a SARRP platform following a cone-beam CT (left panel) with a single prescribed isocenter and beam (center panel). The prescribed dose was 6 Gy and the estimated mean dose using the Muriplan software generated dose volume histogram analysis was 6.25 Gy (right panel). (B). EPR spectroscopic analysis of 500 nM FMX following 6 Gy irradiation using the prescribed treatment plan. (C). EPR spectroscopic analysis of 500 nM FMX following 10 and 20 Gy irradiation using the SARRP system.

4. Discussion

The overarching goal of this study was to test the viability of magnetite iron oxide nanoparticles for radiation dosimetry. The driving principle behind this study is the understanding that ionizing radiation can oxidize the Fe^{2+} sites in the Fe_3O_4 core, facilitating the release of free Fe^{3+} , an effect that is detectable using EPR spectroscopy [18]. This study first showed that xylenol orange is unable to detect free Fe^{3+} release from FMX following irradiation. This is likely due to the low amounts of Fe^{3+} released, which have been shown to be in the order of ≈ 200 nM. These concentrations of released iron are most likely below the limit of detection for xylenol orange, which typically detects iron oxidation in traditional Fricke dosimeters with ferrous ammonium sulfate concentrations of approximately $300 \mu\text{M}$ [23]. At minimum, this study successfully replicated previous results showing that EPR spectroscopy can detect FMX oxidation. The previous study where this was discovered showed radiation dose linearity with 50 nM up to 10 Gy [18]. From this study, linearity up to 20 Gy was not observed with 150 nM FMX but could be observed with 500 nM. These results suggest that surface charge availability is a major limiting factor in detecting radiation-induced oxidation. Therefore, these data warrant consideration of iron oxide nanoparticles with variable sizes, as nanoparticles can range from 5–100 nm. As it has previously been reported that H_2O_2 drives the radiolytic oxidation of Fe_3O_4 [18], the physiochemical properties of the SPIONs themselves should be considered, as positively charged SPIONs have been shown to more readily interact with H_2O_2 [24]. Moving forward, using EPR spectroscopy to assess radiolytic changes to SPIONs is an important tool due to its ease of use and high sensitivity, as observed in this study. Several other clinically relevant dosimetric techniques have relied on EPR spectroscopy (e.g., alanine and lithium formate), which provide significantly greater sensitivity than colorimetric techniques [5,25,26]. Therefore, if the physiochemical properties of SPIONs can be optimized for dosimetric purposes, EPR spectroscopic analysis will provide a sensitive and reliable outlet for clinical purposes.

This study revealed that FMX was unable to adequately estimate the dose from a SARRP system. The dose was underestimated by approximately 4.63 Gy ($\approx 79\%$). This is likely due to the high sensitivity of FMX radiolytic oxidation to changes in dose rate.

Previously, it has been shown that the radiolytic yield of FMX is maximum at 0.6 Gy min^{-1} and decreases linearly as a function of dose rate [18]. Therefore, the higher dose rate of the SARRP ($\approx 2.5 \text{ Gy min}^{-1}$) is suboptimal and provides a significant dose underestimation. Thus, the high sensitivity to changes in dose rate appears to be a significant limiting factor for the use of iron oxides in radiation dosimetry. Based on these results, while the high stability of FMX among other forms of Fe_3O_4 nanoparticles are attractive for use in pre-clinical radiation dosimetry, further investigation into the non-trivial radiochemical properties of SPIONs are required before considering them for this application and may enhance their utility in more therapeutic settings.

5. Conclusions

Overall, this study was able to confirm the utility of electron paramagnetic resonance spectroscopy to assess the radiolytic oxidation of FMX nanoparticles. Despite this fact, FMX SPIONs show limited utility for dose estimation and appear to underestimate doses. This is likely due to their high dose-rate sensitivity. Future research into the unique radiochemical properties of SPIONs is required to assess broader applications.

Author Contributions: Conceptualization, methodology, software, validation, formal analysis, investigation N.R.K. and M.S.P.; resources, M.S.P.; data curation, writing—original draft preparation, writing—review and editing, visualization N.R.K. and M.S.P., supervision, M.S.P.; project administration, M.S.P.; funding acquisition, M.S.P. All authors have read and agreed to the published version of the manuscript.

Funding: This work was supported by NIH grant R21CA270742 and the Radiation Research Foundation (L998500-G).

Data Availability Statement: The data presented in this study are available in this article.

Acknowledgments: The content is solely the responsibility of the authors and does not represent the views of the National Institutes of Health. Core facilities were supported in part by the Carver College of Medicine and the Holden Comprehensive Cancer Center, NIH P30 CA086862.

Conflicts of Interest: The authors declare no conflicts of interest.

References

1. Fricke, H.; Morse, S. The Chemical Action of Roentgen Rays on Dilute Ferrosulphate Solutions as a Measure of Dose. *Am. J. Roentgenol. Radium Ther. Nucl. Med.* **1927**, *18*, 430–432.
2. Mehdi, Z.; Petronek, M.S.; Stolwijk, J.M.; Mapuskar, K.A.; Kalen, A.L.; Buettner, G.R.; Cullen, J.J.; Spitz, D.R.; Buatti, J.M.; Allen, B.G. Utilization of Pharmacological Ascorbate to Enhance Hydrogen Peroxide-Mediated Radiosensitivity in Cancer Therapy. *Int. J. Mol. Sci.* **2021**, *22*, 10880. [[CrossRef](#)] [[PubMed](#)]
3. Schreiner, L.J. Review of Fricke Gel Dosimeters. *J. Phys. Conf. Ser.* **2004**, *3*, 9–21. [[CrossRef](#)]
4. Alpen, E.L. Chapter 6—Radiation Chemistry. In *Radiation Biophysics*, 2nd ed.; Alpen, E.L., Ed.; Academic Press: San Diego, CA, USA, 1998; pp. 104–131. ISBN 978-0-12-053085-4.
5. Yang, Z.; Vrielinck, H.; Jacobsohn, L.G.; Smet, P.F.; Poelman, D. Passive Dosimeters for Radiation Dosimetry: Materials, Mechanisms, and Applications. *Adv. Funct. Mater.* **2024**, 2406186. [[CrossRef](#)]
6. deAlmeida, C.E.; Ochoa, R.; de Lima, M.C.; David, M.G.; Pires, E.J.; Peixoto, J.G.; Salata, C.; Bernal, M.A. A Feasibility Study of Fricke Dosimetry as an Absorbed Dose to Water Standard for ^{192}Ir HDR Sources. *PLoS ONE* **2014**, *9*, e115155. [[CrossRef](#)]
7. Liosi, G.M.; Dondi, D.; Vander Griend, D.A.; Lazzaroni, S.; D’Agostino, G.; Mariani, M. Fricke-Gel Dosimeter: Overview of Xylenol Orange Chemical Behavior. *Radiat. Phys. Chem.* **2017**, *140*, 74–77. [[CrossRef](#)]
8. Valente, M.; Molina, W.; Silva, L.C.; Figueroa, R.; Malano, F.; Pérez, P.; Santibañez, M.; Vedelago, J. Fricke Gel Dosimeter with Improved Sensitivity for Low-Dose-Level Measurements. *J. Appl. Clin. Med. Phys.* **2016**, *17*, 402–417. [[CrossRef](#)]
9. Buglewicz, D.J.; Banks, A.B.; Hirakawa, H.; Fujimori, A.; Kato, T.A. Monoenergetic 290 MeV/n Carbon-Ion Beam Biological Lethal Dose Distribution Surrounding the Bragg Peak. *Sci. Rep.* **2019**, *9*, 6157. [[CrossRef](#)]
10. Toth, G.B.; Varallyay, C.G.; Horvath, A.; Bashir, M.R.; Choyke, P.L.; Daldrup-Link, H.E.; Dosa, E.; Finn, J.P.; Gahramanov, S.; Harisinghani, M.; et al. Current and Potential Imaging Applications of Ferumoxytol for Magnetic Resonance Imaging. *Kidney Int.* **2017**, *92*, 47–66. [[CrossRef](#)]
11. Neuwelt, E.A.; Fu, R.; Gahramanov, S.; Gultekin, S.H.; Lacy, C.; Nasser, M.; Prola Netto, J.; Tyson, R.M.; White, T.; Woltjer, R.L.; et al. Diagnosis of Pseudoprogression Using Ferumoxytol Perfusion MRI in Patients with Glioblastoma to Predict Better Outcome. *J. Clin. Oncol.* **2014**, *32*, 2010. [[CrossRef](#)]

12. Gahramanov, S.; Varallyay, C.; Tyson, R.M.; Lacy, C.; Fu, R.; Netto, J.P.; Nasser, M.; White, T.; Woltjer, R.L.; Gultekin, S.H.; et al. Diagnosis of Pseudoprogression Using MRI Perfusion in Patients with Glioblastoma Multiforme May Predict Improved Survival. *CNS Oncol.* **2014**, *3*, 389–400. [[CrossRef](#)] [[PubMed](#)]
13. Ramanathan, R.K.; Korn, R.L.; Raghunand, N.; Sachdev, J.C.; Newbold, R.G.; Jameson, G.; Fetterly, G.J.; Prey, J.; Klinz, S.G.; Kim, J.; et al. Correlation between Ferumoxytol Uptake in Tumor Lesions by MRI and Response to Nanoliposomal Irinotecan in Patients with Advanced Solid Tumors: A Pilot Study. *Clin. Cancer Res.* **2017**, *23*, 3638. [[CrossRef](#)] [[PubMed](#)]
14. Barajas, R.F., Jr.; Hamilton, B.E.; Schwartz, D.; McConnell, H.L.; Pettersson, D.R.; Horvath, A.; Szidonya, L.; Varallyay, C.G.; Firkins, J.; Jaboin, J.J.; et al. Combined Iron Oxide Nanoparticle Ferumoxytol and Gadolinium Contrast Enhanced MRI Define Glioblastoma Pseudoprogression. *Neuro-Oncology* **2018**, *21*, 517–526. [[CrossRef](#)] [[PubMed](#)]
15. Coyne, D.W. Ferumoxytol for Treatment of Iron Deficiency Anemia in Patients with Chronic Kidney Disease. *Expert Opin. Pharmacother.* **2009**, *10*, 2563–2568. [[CrossRef](#)] [[PubMed](#)]
16. Trujillo-Alonso, V.; Pratt, E.C.; Zong, H.; Lara-Martinez, A.; Kaittanis, C.; Rabie, M.O.; Longo, V.; Becker, M.W.; Roboz, G.J.; Grimm, J.; et al. FDA-Approved Ferumoxytol Displays Anti-Leukaemia Efficacy against Cells with Low Ferroportin Levels. *Nat. Nanotechnol.* **2019**, *14*, 616–622. [[CrossRef](#)] [[PubMed](#)]
17. Zanganeh, S.; Hutter, G.; Spitler, R.; Lenkov, O.; Mahmoudi, M.; Shaw, A.; Pajarinen, J.S.; Nejadnik, H.; Goodman, S.; Moseley, M.; et al. Iron Oxide Nanoparticles Inhibit Tumour Growth by Inducing Pro-Inflammatory Macrophage Polarization in Tumour Tissues. *Nat. Nanotechnol.* **2016**, *11*, 986–994. [[CrossRef](#)]
18. Petronek, M.S.; Spitz, D.R.; Buettner, G.R.; Allen, B.G. Oxidation of Ferumoxytol by Ionizing Radiation Releases Iron. An Electron Paramagnetic Resonance Study. *J. Radiat. Res.* **2022**, *63*, 378–384. [[CrossRef](#)]
19. Petronek, M.S.; Teferi, N.; Caster, J.M.; Stolwijk, J.M.; Zaher, A.; Buatti, J.M.; Hasan, D.; Wafa, E.I.; Salem, A.K.; Gillan, E.G.; et al. Magnetite Nanoparticles as a Kinetically Favorable Source of Iron to Enhance GBM Response to Chemoradiosensitization with Pharmacological Ascorbate. *Redox Biol.* **2023**, *62*, 102651. [[CrossRef](#)]
20. Gambarini, G.; Liosi, G.M.; Artuso, E.; Giacobbo, F.; Mariani, M.; Brambilla, L.; Castiglioni, C.; Carrara, M.; Pignoli, E. Study of the Absorption Spectra of Fricke Xylenol Orange Gel Dosimeters. In Proceedings of the 2015 4th International Conference on Advancements in Nuclear Instrumentation Measurement Methods and their Applications (ANIMMA), Lisbon, Portugal, 20–24 April 2015; pp. 1–5.
21. Scotti, M.; Arosio, P.; Brambilla, E.; Gallo, S.; Lenardi, C.; Locarno, S.; Orsini, F.; Pignoli, E.; Pedicone, L.; Veronese, I. How Xylenol Orange and Ferrous Ammonium Sulphate Influence the Dosimetric Properties of PVA–GTA Fricke Gel Dosimeters: A Spectrophotometric Study. *Gels* **2022**, *8*, 204. [[CrossRef](#)]
22. Zaher, A.; Duchman, B.; Ivanovic, M.; Spitz, D.R.; Furqan, M.; Allen, B.G.; Petronek, M.S. Exploratory Analysis of Image-Guided Ionizing Radiation Delivery to Induce Long-Term Iron Accumulation and Ferritin Expression in a Lung Injury Model: Preliminary Results. *Bioengineering* **2024**, *11*, 182. [[CrossRef](#)]
23. Rousseau, A.; Stien, C.; Bordy, J.-M.; Blideanu, V. Fricke-Xylenol Orange-Gelatin Gel Characterization with Dual Wavelength Cone-Beam Optical CT Scanner for Applications in Stereotactic and Dynamic Radiotherapy. *Phys. Medica Eur. J. Med. Phys.* **2022**, *97*, 1–12. [[CrossRef](#)] [[PubMed](#)]
24. Javanbakht, T.; Laurent, S.; Stanicki, D.; Frenette, M. Correlation between Physicochemical Properties of Superparamagnetic Iron Oxide Nanoparticles and Their Reactivity with Hydrogen Peroxide. *Can. J. Chem.* **2020**, *98*, 601–608. [[CrossRef](#)]
25. Höfel-Pessies, S.; Stehle, M.; Zwicker, F.; Fix, M.; Drescher, M. A Practical EPR Dosimetry System for Routine Use in Radiotherapy: Uncertainty Analysis of Lithium Formate Dosimeters at the Therapeutic Dose Level. *Phys. Med. Biol.* **2021**, *66*, 045005. [[CrossRef](#)]
26. Helt-Hansen, J.; Rosendal, F.; Kofoed, I.M.; Andersen, C.E. Medical Reference Dosimetry Using EPR Measurements of Alanine: Development of an Improved Method for Clinical Dose Levels. *Acta Oncol.* **2009**, *48*, 216–222. [[CrossRef](#)] [[PubMed](#)]

Disclaimer/Publisher’s Note: The statements, opinions and data contained in all publications are solely those of the individual author(s) and contributor(s) and not of MDPI and/or the editor(s). MDPI and/or the editor(s) disclaim responsibility for any injury to people or property resulting from any ideas, methods, instructions or products referred to in the content.